

Effects of Rotating Tabs on Flow and Acoustic Fields of Supersonic Jet

Mohammed K. Ibrahim* and Yoshiaki Nakamura†
Nagoya University, Nagoya 464-8603, Japan

I. Introduction

OVER the past 20 years, many researchers have investigated the effects of delta tabs and simple rectangular tabs on both circular and rectangular jets¹⁻⁴ in an attempt to enhance jet mixing and to reduce jet noise. Those tabs are characterized by producing a pair of counter-rotating vortices with a sense of rotation opposite to that expected from the wrapping of the nozzle boundary layer.³ In the studies, the jet cross section could be distorted in a variety of ways, depending on the number and placement of the tabs.

In the present paper, the effects of freely rotating vane-type tabs on jet and its emitted sound are the main subjects. The tabs, which are supported by bearings, are allowed to rotate freely around the jet axis. The jet flow generates an aerodynamic force on part of the vane portion that is protruded inside the jet. This force causes the vanes to rotate around the jet axis. The vane-type tab is characterized by producing a single trailing vortex. When those vanes are placed at diametrically opposite locations along the circumference of a nozzle exit such that the vortices produced by the vanes have the same sense of rotation, then the torque produced by each vane is summed. This configuration, which is referred to as the rotating vane tabs hereafter, is shown schematically in Fig. 1a. Stationary vane tabs shown in Fig. 1b are investigated for comparison.

II. Tab Geometry

In the vane-type tab configuration employed here, each vane has a rectangular cross section with a thickness to chord ratio t/c of 0.33. The protrusion ratio is w/D , where w is the protrusion height into the jet flow and D is the nozzle exit diameter. Two cases for this ratio, $w/D = 6.4$ and 12.8%, are studied. The supersonic nozzle has an exit diameter of 7.8 mm and a throat diameter of 7.5 mm, with a design Mach number M_D of 1.33. The area blockage is due to tabs percent area blockage $= (A_{\text{without tab}} - A_{\text{with tab}}) / A_{\text{without tab}} \times 100$, which is a function of w/D and vane angle, α_v . The area blockage due to each vane is 2% for the case where $w/D = 6.4\%$ and $\alpha_v = 30$ deg.

III. Results

All experiments were conducted in the open jet facility at the Fluid Dynamics Laboratory, Department of Aerospace Engineering, Nagoya University. Detailed description of the facility may be found in Ref. 5. To represent a supersonic jet, the fully expanded Mach number M_j is commonly used. It is uniquely related to the nozzle pressure ratio P_{t0}/P_a through the following equation:

$$M_j = \left\{ \left[(P_{t0}/P_a)^{(\gamma-1)/\gamma} - 1 \right] 2/(\gamma-1) \right\}^{0.5} \quad (1)$$

where P_{t0} is the chamber pressure or the jet total pressure and P_a is the ambient pressure. Most of the results are presented here for $P_{t0}/P_a = 5$, which corresponds to $M_j = 1.71$.

A. Jet Spreading

A large increase in jet spreading under the influence of tabs is indicated in Fig. 2a for both stationary and rotating configurations with four vanes, where $w/D = 6.4\%$ and $\alpha_v = 30$ deg. The pressure measured in supersonic flow region represents the pitot pressure P_{t2} ,

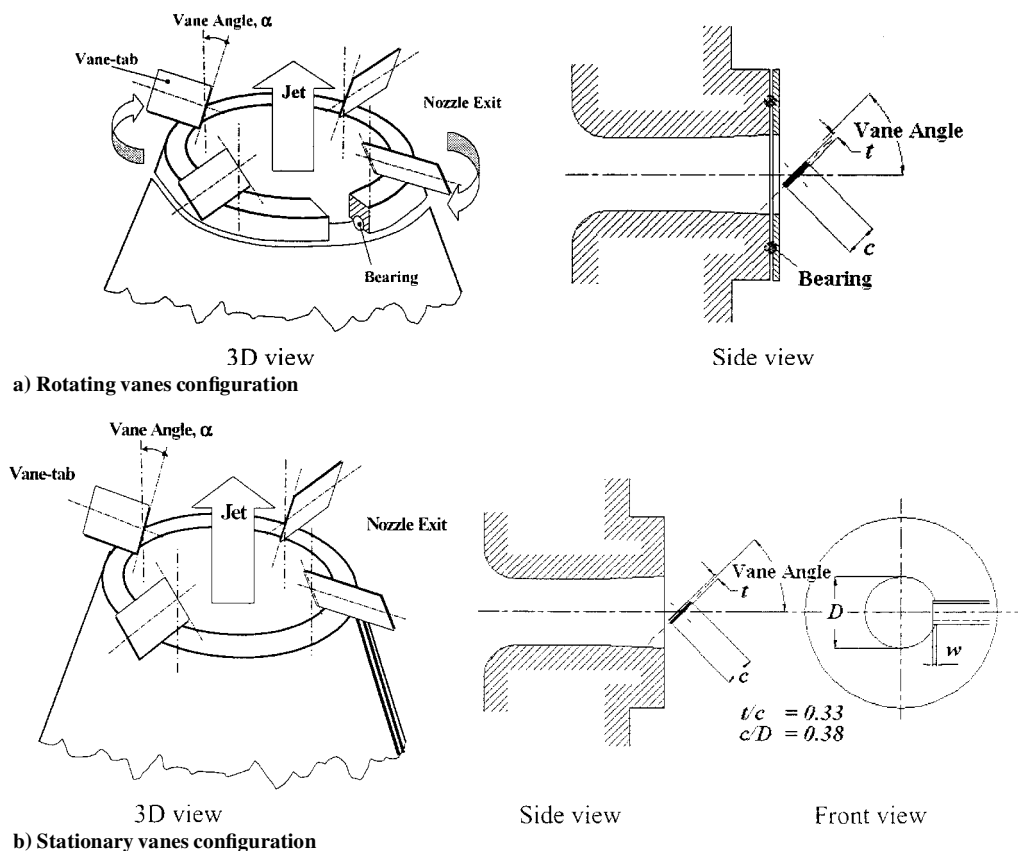
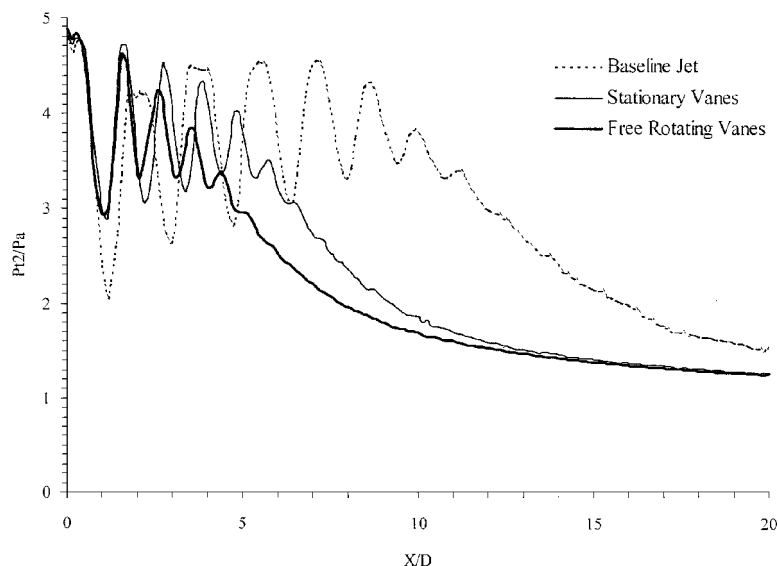
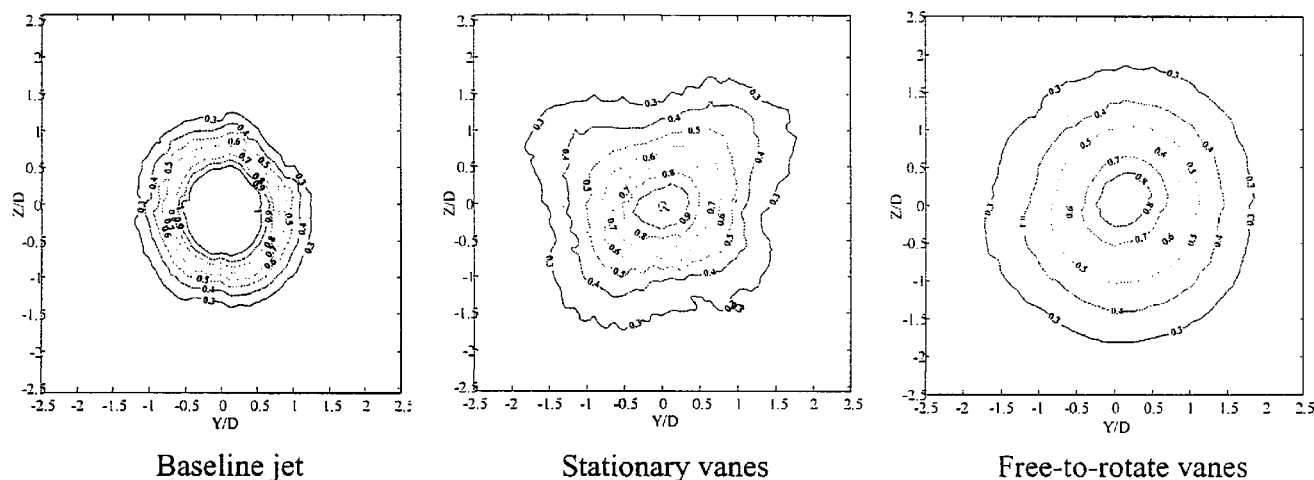


Fig. 1 Schematic of vane-type tabs.



a) Centerline distribution of stagnation pressure normalized by ambient pressure



b) Mach number contours at $x/D = 10$

Fig. 2 Effects of four vanes: $w/D = 6.4\%$, $\alpha_v = 30$ deg, and $M_j = 1.71$.

that is, the pressure downstream of the standing bow shock produced by a pitot probe itself.

Those results show wavy pressure patterns due to the standing shock/expansion structure inside the jet. The tabs can weaken the shock/expansion structure dramatically. The jet centerline stagnation pressure and, thus, the Mach number are found to decay much faster than those of the baseline jet, which suggests an increase in jet spreading. The rotating vanes can make the jet decay faster and the shock/expansion structure weaker than the corresponding stationary configuration. The maximum rotational speed of the rotating vanes was about 130 revolutions per second.

Mach number distributions on jet cross-sectional planes were measured with a pitot tube. These data were collected for enough downstream to assume that the flow was subsonic everywhere and that the static pressure had been relaxed to the ambient pressure.³ Hence, the Mach number can be calculated reliably from only the pitot tube measurement data. Figure 2b shows Mach number contours at $x/D = 10$ for three cases: the baseline jet and the stationary and the rotating cases with four vanes. The enormous effects of those tabs on jet spreading can be readily appreciated. The jet plume cross section maintains an axisymmetric shape for the case of the rotating vanes, although it becomes asymmetric for the case of the stationary vanes.

Figure 3a shows the case with two vanes, where $w/D = 12.8\%$ and $\alpha_v = 30$ deg, as well as the baseline jet. In this case, it is seen that the stationary case has a higher jet spreading rate than the rotating case. Note that the distributions along the centerline do not always represent actual jet spreading. From Fig. 3b, where the Mach number

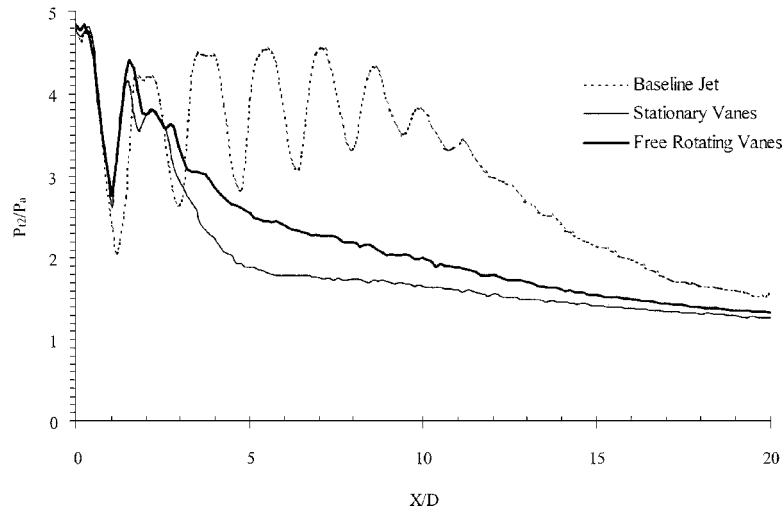
contours at $x/D = 5$ are shown for these cases, note that the jet in the stationary case is essentially bifurcated. Zaman et al.⁴ also have observed a similar effect by using two delta tabs with a sonic nozzle.

B. Jet Noise

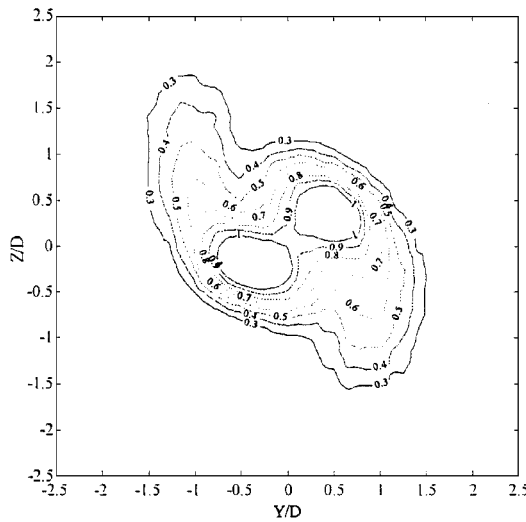
The far-field noise spectra in the case of four vanes with $\alpha_v = 30$ deg and $w/D = 6.4\%$ are shown for both stationary and rotational configurations in Fig. 4, where a microphone was placed at a distance of $100D$ and at an angle of 90 deg from the jet axis. The baseline jet spectra are also presented in Fig. 4 for comparison, and they are clearly characterized by a screech tone. The fundamental frequency is about 12.7 kHz. The noise spectra of both rotating and stationary cases are quite similar in characteristics. The sound pressure level (SPL) for these cases is reduced over an audible frequency range, compared with that of the baseline jet, where the screech components are eliminated. On the other hand, the SPL for higher frequencies is slightly increased. This increase was also observed by Norum and Seiner,⁶ who made an attempt to suppress screech tones in convergent-divergent nozzles. According to their explanation, the tab induces a secondary shock structure, which produces undesirable noise at high frequencies. Although it was expected that the spectra of rotating vanes would be decreased more than the stationary vanes because the former has a relatively higher spreading rate than the latter, as shown in Fig. 2, they actually showed almost the same noise level.

C. Jet Thrust

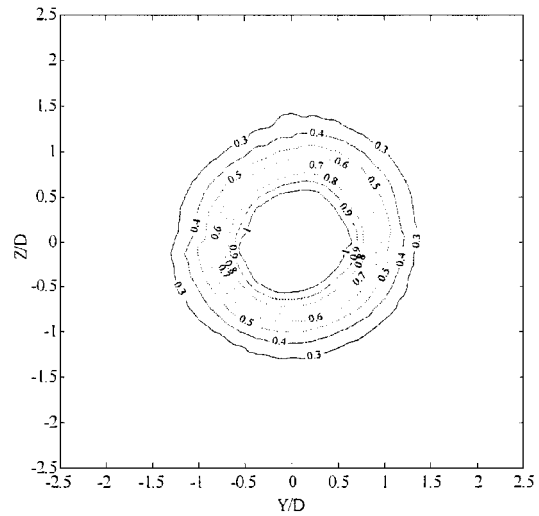
Thrust is a function of nozzle pressure ratio (NPR). Figure 5 shows the NPR results for both the stationary and the rotating



a) Centerline distribution of stagnation pressure normalized by ambient pressure



a. Stationary vanes



b. Free rotating vanes

b) Mach number contours at $x/D = 5$

Fig. 3 Effects of two vanes: $w/D = 12.8\%$, $\alpha_v = 30$ deg, and $M_j = 1.71$.

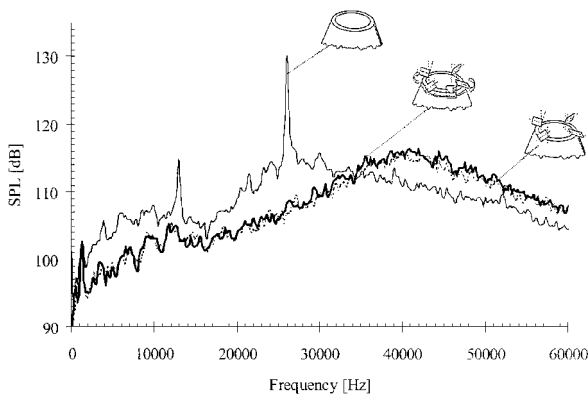


Fig. 4 Far-field SPL spectra for $M_j = 1.71$: —, baseline jet; —, rotating vanes; and ---, stationary vanes.

cases, with four vanes, where $\alpha_v = 30$ deg and $w/D = 6.4\%$. In Fig. 5, an isentropic prediction is also presented, which is given by

$$\text{thrust} = (P_e - P_a)A_e + P_e A_e \gamma M_e^2 \quad (2)$$

where M_e is the Mach number, A_e is the exit area, P_e is the static pressure at the nozzle exit, and γ is the ratio of specific heat for air.

Good agreement between the baseline jet and the isentropic prediction in the underexpanded region, that is, $\text{NPR} \geq 3$, validates the

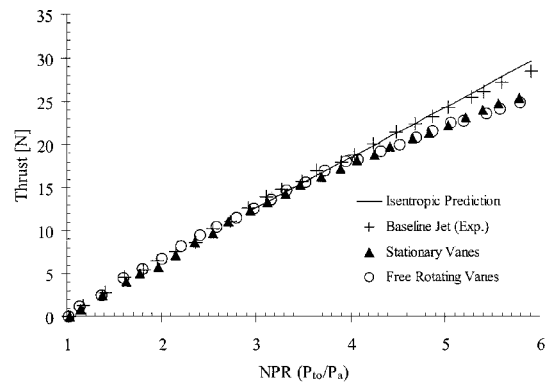


Fig. 5 Jet thrust vs. NPR.

accuracy of the present measurement. Furthermore, it turns out that both stationary and rotating cases have almost the same amount of thrust penalty. For $\text{NPR} = 5$, the loss is about 6.9% as large as that of the baseline jet, which corresponds to about 1.5–2% per vane. Generally, the thrust loss increases with w/D . Although the rotating vanes have almost the same thrust penalty as the stationary vanes, the rotating vanes seem to be advantageous over the stationary vanes because the former have a higher jet spreading rate than the latter.

IV. Summary

A new configuration of vortex generator has been proposed. This vortex generator, referred to as vane-type tab, can freely rotate around the jet axis. The effects of rotation on flow and acoustic fields, as well as thrust penalty, were investigated. A higher jet-spreading rate for the decay of the centerline velocity can be achieved compared with the corresponding stationary vanes. The jet plume cross section maintains an axisymmetric shape for the rotating case, whereas it is often nonaxisymmetric for the stationary case, depending on the number of vanes and their azimuthal locations. The rotation does not increase the noise level, and it does not impose larger thrust penalty either, compared with the stationary case. The vanes can reduce the overall SPL by as much as 10 dB in both cases, whereas the thrust penalty is about 1.5–2% per vane.

References

- ¹Ahuja, K. K., and Brown, W. H., "Shear Flow Control by Mechanical Tabs," AIAA Paper 89-0994, 1989.
- ²Zaman, K. B. M. Q., "Spreading Characteristics of Compressible Jets from Nozzles of Various Geometries," *Journal of Fluid Mechanics*, Vol. 383, 1999, pp. 197–228.
- ³Samimy, M., Zaman, K. B. M. Q., and Reeder, M. F., "Effect of Tabs at the Nozzle Lip on the Flow and Noise Field of an Axisymmetric Jet," *AIAA Journal*, Vol. 31, 1993, pp. 609–619.
- ⁴Zaman, K. B. M. Q., Reeder, M. F., and Samimy, M., "Control of an Axisymmetric Jet Using Vortex Generator," *Physics of Fluids*, Vol. 6, No. 2, 1994, pp. 778–793.
- ⁵Ibrahim, M. K., and Nakamura, Y., "Flowfield and Noise Characteristics due to Supersonic Jet Shear-Layer Vortex Interaction," AIAA Paper 2000-2533, 2000.
- ⁶Norum, T. D., and Seiner, J. M., "Experiments on Shock Associated Noise of Supersonic Jets," AIAA Paper 79-1526, 1979.

M. Samimy
Associate Editor

Multiple Sensor Control of Vortex Shedding

E. A. Gillies*

University of Glasgow, Scotland G12 8QQ,
United Kingdom

Introduction

MANY wake flows exhibit self-excited flow oscillations that are sustained by the flow itself and are not caused by amplification of external noise. The archetypal example of a self-excited wake flow is the unsteady flow past a circular cylinder. This flow exhibits self-sustained periodic vortex shedding above a critical Reynolds number. Suppression of vortex shedding, by flow control, is desirable to mitigate flow-induced structural vibrations and reduce drag and aerodynamic noise. However, controlling any fluid flowfield is a difficult task—the governing Navier–Stokes equations are nonlinear and have infinite degrees of freedom. The control problem is further complicated by the fact that fluid flows often evolve spatially and incorporate inherent time delays between control actuation and response. In this Note control is taken to mean complete suppression of flow oscillations.

In an actual cylinder wake the flow is three dimensional. However, it is reasonable to assert that control of the idealized two-dimensional wake must be demonstrated before associated three-dimensional instabilities are addressed. (Vortex shedding at start up is always two dimensional.^{1,2}) This Note only considers feedback stabilization of the idealized two-dimensional cylinder wake and is only applicable

to the very low-Reynolds-number range (<190) where the wake is two-dimensional, and also for cylinders of short span. Roussopoulos and Monkewitz³ showed that two-dimensional models of vortex shedding with single sensor feedback are only appropriate for short spans ($<30D$) such that the span between the feedback sensor and either end is less than a critical length; otherwise, shedding is reestablished at other spanwise locations as a result of end effects.

The appropriate control strategy for any fluid flow depends on the nature of the fluid flow instability. In the low-Reynolds-number flow past a two-dimensional circular cylinder, the mean flow velocity profiles in the near wake are absolutely unstable, and this entire region acts as a "wavemaker" for the vortex street.⁴ Absolutely unstable flows are intrinsically unstable and demonstrate self-excited oscillations even when all sources of noise are removed. These absolutely unstable flows present difficulties for flow control as they are relatively insensitive to external forcing and often interact with the control in a nonlinear fashion.¹

Because the flow is inherently unstable, the enhancement of vortex shedding using a single sensor-actuator feedback loop is relatively straightforward. However, the suppression of vortex shedding by active control is much more difficult. As the Reynolds number is increased, the region of absolute instability in the near wake grows, and more and more global modes can become unstable. Although the von Kármán mode is the first global mode to become unstable, a wake flow can possess multiple global modes. Control of the flow requires attenuation of all of these global modes.²

Complete suppression of vortex shedding is feasible using a single sensor at slightly supercritical Reynolds numbers ($Re < 60$ from tunnel experiments of Ref. 5 or $Re < 80$ in a numerical experiment of Ref. 6). Farther beyond the critical value, however, the forcing amplitude necessary to control the most unstable mode merely destabilizes the next most unstable mode.^{2,5} Oscillations can be suppressed at the sensor location but are, in general, exacerbated elsewhere.⁵ Single-sensor linear feedback control is not an appropriate control strategy for the two-dimensional circular cylinder wake.

Wake Model

A numerical model of the circular cylinder wake with control feedback was required to investigate various alternative control strategies. An appropriate flow model is the one-dimensional, complex Ginzburg–Landau (G–L) equation,^{2,7} which contains all of the stability features of the two-dimensional cylinder wake pertinent to control.^{2,7} This wake model has been used frequently in the literature for wake control studies and has been shown to allow semiquantitative predictions of the wake with feedback.² Significantly, the G–L model demonstrates the ineffectiveness of single-sensor feedback in controlling the wake past a critical Reynolds number⁷: like the cylinder wake it has many unstable global modes. The G–L model is, however, relatively straightforward to integrate numerically and allows rapid prototyping of control strategies.

The wake model chosen for the study was of the following form⁷:

$$\frac{\partial A}{\partial t} + U \frac{\partial A}{\partial x} = \mu(x)A + (1 + jc_d) \frac{\partial^2 A}{\partial x^2} - (1 + jc_n)|A|^2 A$$

where $A(x, t)$ is the complex amplitude and U , c_d , c_n , and $\mu(x)$ are real. With fixed advection speed U and fixed parameter c_d the stability of the G–L wake is defined by the growth rate parameter $\mu(x) = \mu_0 + \mu'x$, where μ_0 is similar to a Reynolds number based on the cylinder diameter.⁷ For $\mu' < 0$ the stability features of this prototype wake are similar to the stability features of a two-dimensional cylinder wake. Like a low-Reynolds-number cylinder wake, the G–L wake is absolutely unstable near the origin where $\mu(x) > U^2/4(1 + c_d^2)$, convectively unstable further downstream where $0 < \mu(x) < U^2/4(1 + c_d^2)$, and ultimately stable far downstream. Like the cylinder wake, the G–L model becomes globally unstable and oscillates with a coherent frequency when the region of absolute instability reaches a critical size.

The G–L model was solved numerically on a domain with $0 < x < 120$ using 1000 grid points with boundary conditions $A(0, t) = 0$ (which simulates the cylinder body) and $A(120, t) = 0$. The local growth rate $\mu(x)$ varies linearly in the streamwise direction such that the flow becomes stable far downstream. For all of

Received 19 April 2000; presented as Paper 2000-1933 at the AIAA/CEAS 6th Aeronautics Conference, Lahaina, HI, 12 June 2000; revision received 6 September 2000; accepted for publication 27 November 2000. Copyright © 2001 by the American Institute of Aeronautics and Astronautics, Inc. All rights reserved.

*Lecturer, Department of Aerospace Engineering.